Journal of Hazardous Materials, 32 (1992) 1–39
Elsevier Science Publishers B.V., Amsterdam

Shell Stanlow fluoroaromatics explosion — 20 March 1990: Assessment of the explosion and of blast damage

A.T. Cates
Shell Research Ltd, Thornton Research Centre, P.O. Box 1, Chester CH1 3SH (UK)
(Received September 4, 1991; accepted March 9, 1992)

Abstract

At 3.20 a.m., 20 March 1990, a violent explosion at the fluoroaromatics plant in the Shell Stanlow Manufacturing Complex injured six people, destroyed the plant and caused considerable damage to nearby buildings and plant. The level of blast was considerably above that expected from a runaway reaction and vessel rupture. This paper contains a description of the blast damage caused by the explosion, and an analysis of the type of events that might have caused such damage. The chemical mechanisms involved in the runaway reactions are the subject of another paper. The most likely sequence of events is indicated as a vessel rupture followed immediately by a highly congested jet fireball, where a large quantity of flammable material was released at high speed and instantly ignited in a very congested structure.

1. Introduction

At 3.20 a.m. on 20 March 1990, there was an explosion at the fluoroaromatics plant in the Stanlow Manufacturing Complex during the manufacture of difluoroaniline. The explosion was quite energetic. Missiles were thrown up to 500 m away. The fluoroaromatics plant itself was devastated, and nearby buildings suffered serious structural damage. Windows and door frames over 500 m away were damaged. A subsequent xylene fire burned for over an hour. Six people were injured, one of whom died later in hospital from post-operative complications following lower limb surgery. A long secondary fire was caused, involving the inventory of nearby vessels, including four xylene tanks. The secondary fire followed the primary explosion quite quickly.

This paper contains a description of the blast damage, and a discussion of the blast-generating processes involved in the event. The initiating event, which was almost certainly a chemical runaway reaction, is discussed elsewhere [1,2]. The consequences, granted that such an event took place, are discussed in detail here.

Correspondence to: Dr. A.T. Cates, Shell Research Ltd, Thornton Research Centre, P.O. Box 1, Chester CH1 3SH (UK)

2. Blast and missile damage

2.1 General observations

Analysis of the blast damage from the explosion was complicated by both missile damage and fire damage. Examination of the damage was restricted by the precautions necessitated by contamination. The missiles and blast damage were erratic and very directional.

We draw attention to four features of the blast damage:

(1) The damage level decayed very slowly with distance.

(2) The level of damage was at least an order to magnitude too high to be accounted for a simple vessel rupture.

(3) Damage to individual structures showed evidence of a long time duration event.

(4) A lot of the damage was associated with the rarefaction part of the pressure wave.

These features are discussed in detail below. Each of these features is significant in working out the nature of the blast-generating event(s). The nature of the event indicated by these features is discussed in Sections 4 and 5, where other supporting evidence is given.

2.2 Nature of near-field damage and missiles

The distribution of missiles is included in Appendix A and Fig. 3. The near-field damage (within 10 m of the reactor vessel) was severe (Plate 1), and is discussed in more detail in Appendix B and Fig. 1.

The vessel itself was torn into at least three large pieces, with the top piece being flung a considerable distance (200 m). As far as can be worked out from a visual examination of the vessel, the vessel first burst near the top weld, at about 320° with respect to plant north. It was then torn vertically downwards and horizontally around, close to the weld, before the horizontal tears joined up near the top of the vessel. The burst was therefore towards the north-west leg which supported the concrete roof above the reactor vessel. Most plant structure within about 5 m of the vessel was either turned into missiles, or badly buckled. Much of the major structural damage was associated with the collapse of the north-west leg.

The major vessel fragment ended up outside the plant structure, apparently having been propelled north-west. The rupture itself (if we are correct about the orientation of the blast and the vertical tear) would have pushed this piece of vessel into the structure.

A rough estimate of the rupture pressure of the vessel, and of the tear forces, is included in Appendix C. This estimate gives a value of around 60–80 bar for the rupture pressure of the vessel, and is supported by our own metallurgist's report. A detailed examination of the vessel top has been conducted by the UK HSE, but reached different conclusions on the failure pressure.

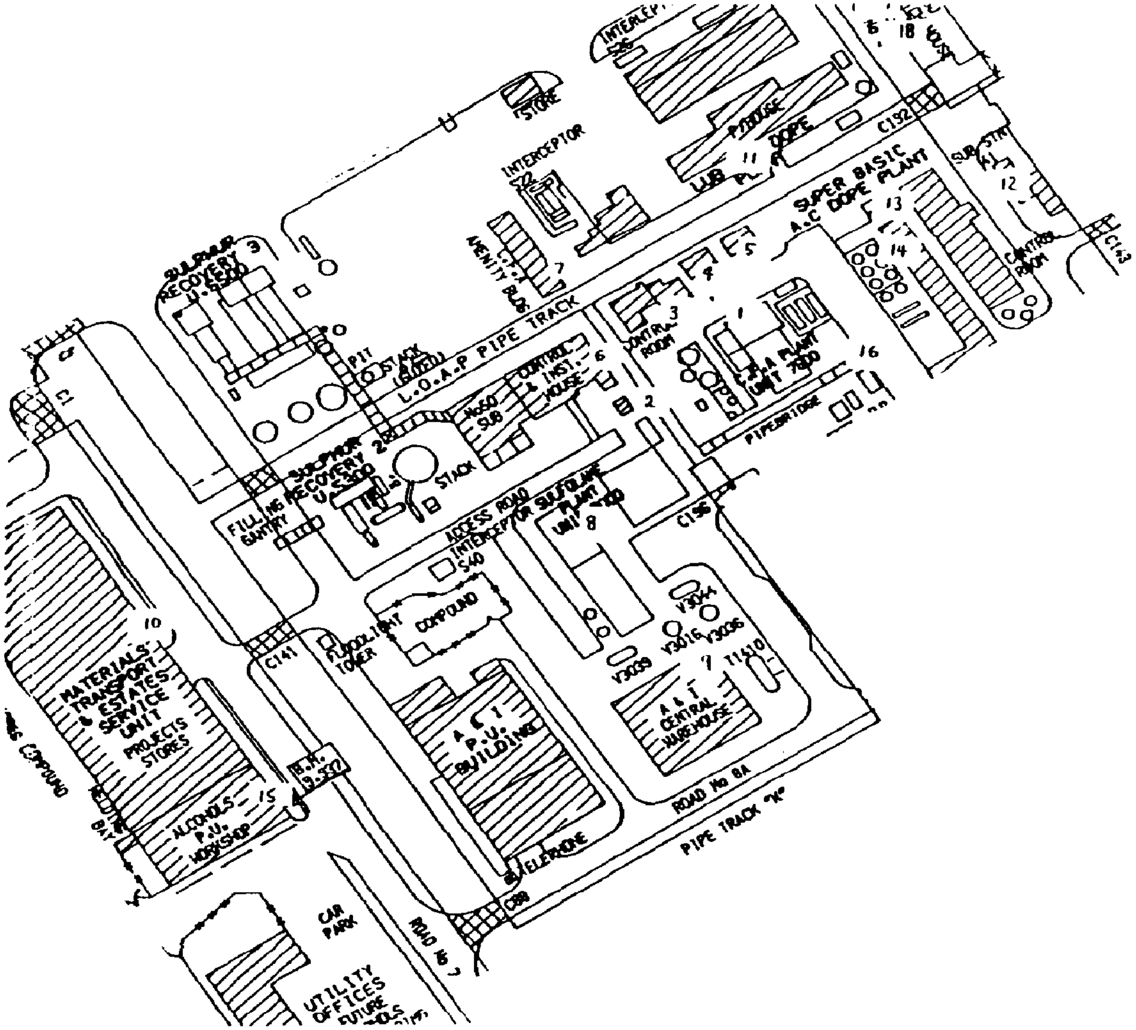

Fig. 1. Map of site damage around CFA plant (see Appendix A).

Missile 47 (Plate 2) is relevant to understanding the nature of the explosion event. This missile was a light fitting which was originally in the neighbourhood of the reactor vessel. Half of this light fitting is badly burnt, and the other half is not damaged. The light fitting was found 75 m away from the explosion, well away from the zone of the subsequent fire. The burning took place before the blast event. Despite the blast, and impact on landing, both the box cover and one glass tube were intact. This missile is discussed in more detail below.

The area behind the plant structure was shielded from missiles by the plant structure, and nearly all the missiles were found within 80° either side of plant north.

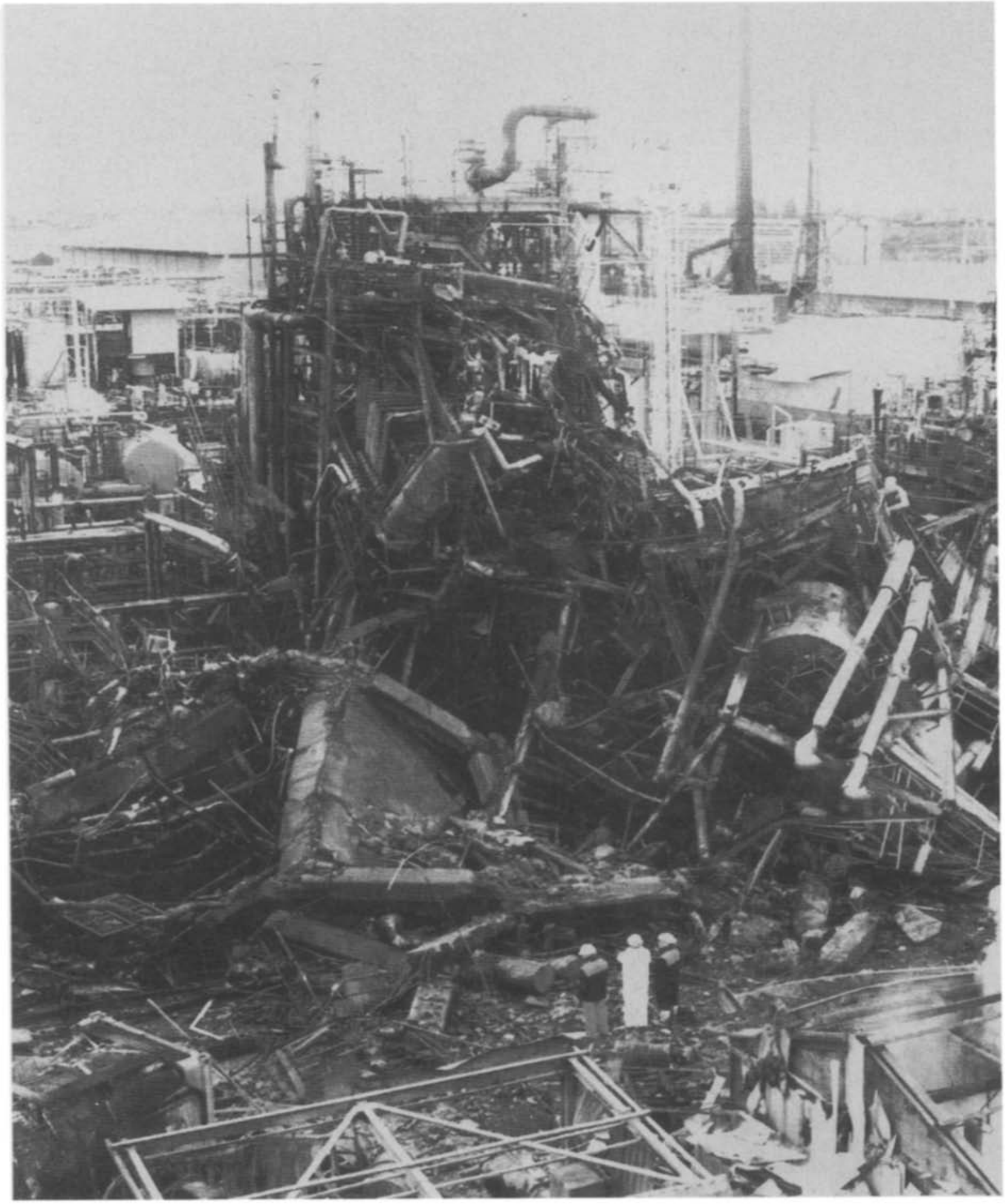

Plate 1. Near-field damage (within 10 m from the reactor).

2.3 Nature of intermediate field damage

The damage in the 10–150 m range is discussed in detail in Appendix B. The damage pattern in this range is very erratic. This was partly because the source

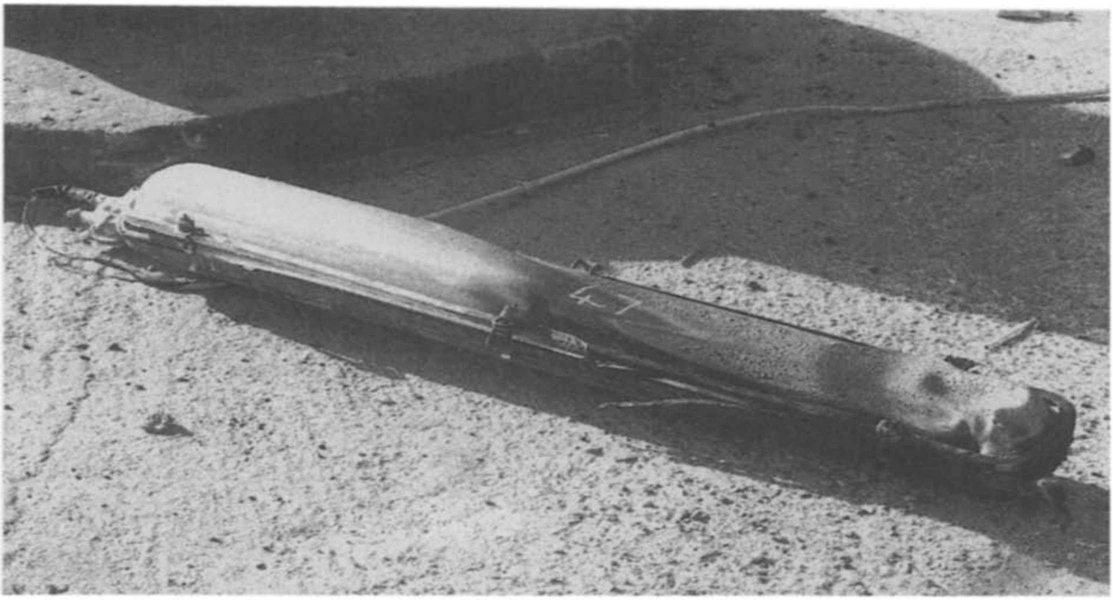

Plate 2. Two burned lightboxes.

of the blast was very directional, and partly because there was a good deal of shielding by plant and other buildings. The pressure field was probably dominated by an aerial hemispherical pressure wave. Most of the medium-field damage was caused by the downward diffraction of this pressure cap.

A plot of the likely pressure required to cause the damage seen versus distance is given in Fig. 2. The erratic level of damage should be noted. It is interesting that, although in the near-field, the highest levels of damage are plant north of the vessel; in the medium and far-field the two major areas of damage (the Materials and Transport Building and Thornton Research Centre) are at 90° in either direction to this.

Many of the pressures estimated (particularly for damage to brittle targets) are taken from TNT (trinitrotoluene) data lists [3]. These are marked as crosses in Fig. 2. Since the pressure pulse that the structures were subjected to was quite different from the spike of a TNT wave, the estimated pressures are likely to be quite different from the actual overpressures exerted. In this regard, the far-field overpressure estimates are likely to represent the pressure that occured more accurately, and the near-field overpressures are likely to be consistently underestimated. There are no reliable data available for the damage caused to brittle structures, such as brick walls, from pressure pulses other

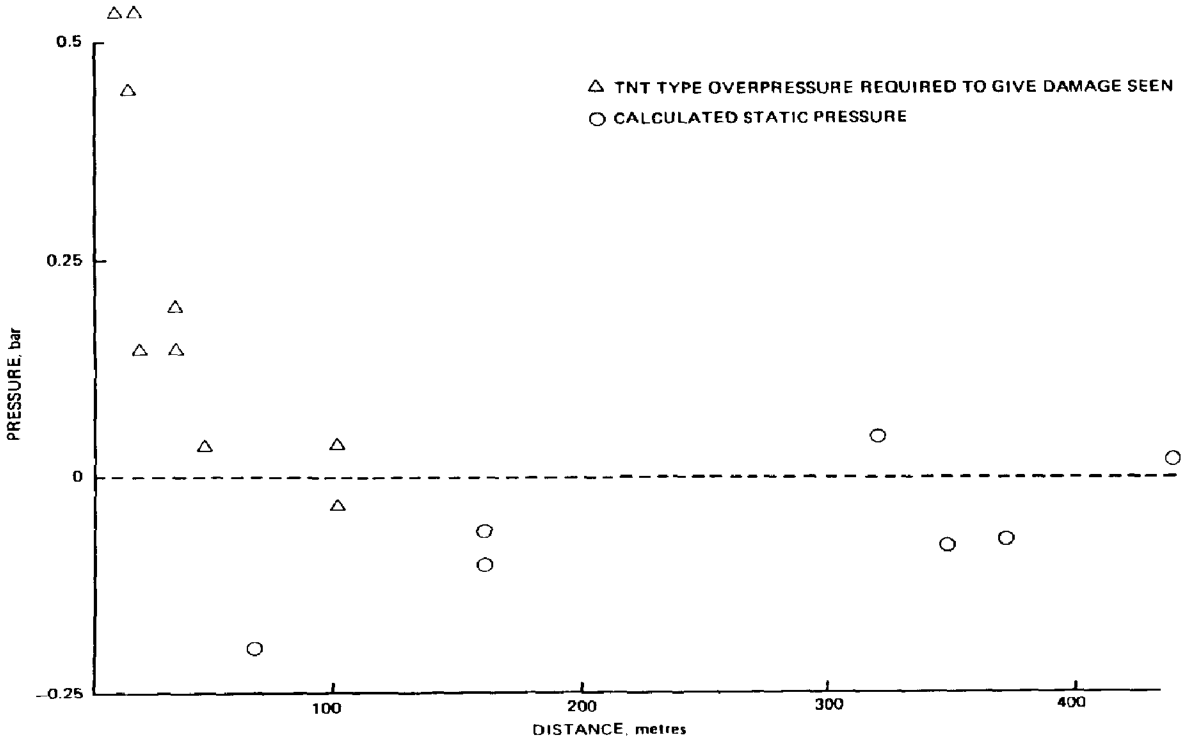

Fig. 2. Pressures required to produce observed damage.

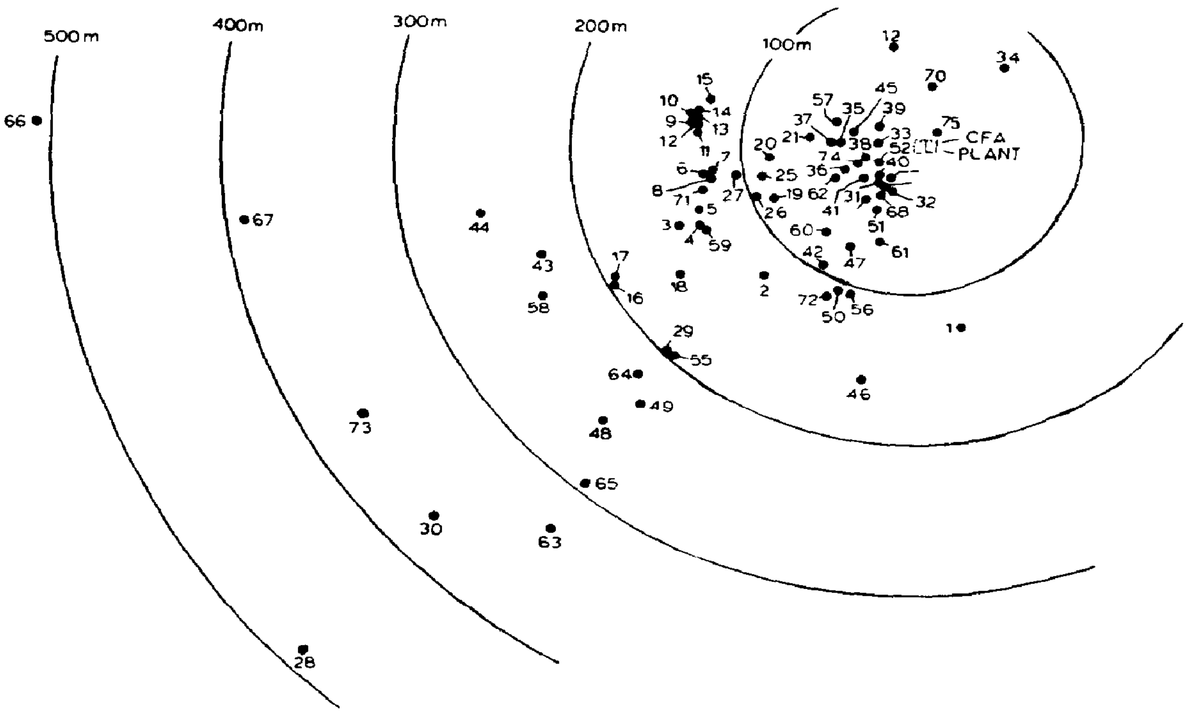

Fig. 3. Map of missile scatter (see also Appendix G for a description of each number).

than TNT or nuclear blast. The pressure loading experienced was generally in the quasistatic, rather than dynamic, response regime.

2.4 Nature of far-field damage

Thornton Research Centre is adjacent to Stanlow Manufacturing Complex, with its boundary about 350 m north-east of the explosion centre. The far-field damage to Thornton Research Centre is detailed in Appendix D. This site was a good indicator of the level of far-field pressure, as it contained a number of relatively sensitive buildings. The near edge of the site was just over 300 m from the explosion centre, and damage on the site extended to more than 500 m from the explosion centre.

The pressure experienced on the Thornton site was undoubtedly aggravated by the site being on slightly raised ground, so that acoustic reflection off the slope increased the level of compression and rarefaction. Even allowing for this effect, the amount of damage at the Research Centre was very high compared to the medium and near-field damage. Weather data supplied by the Meteorological Office rule out the possibility of aggravation by a temperature inversion, since the mixing layer was around 900 m deep.

Two points are drawn from points (2) and (13) in Appendix D. The first is that the duration of the compression phase was, at the very least, 30 ms; and the second is that the far-field shows an energy yield of at least 500 MJ. The actual energy yield must be considerably higher, since we shall argue that the pressure wave was of a very long duration, and therefore a very low "efficiency" event (in TNT efficiency terminology).

A typical far-field energy yield for a long duration event such as a vapour cloud explosion would be a few per cent, which would lead to an estimate of 25 000 MJ released at source. Since this event was unusually long, even compared to that from a vapour cloud explosion, the efficiency is likely to be less than this, and the energy release at source even more.

Although the damage was erratic, some consistent patterns arose. A lot of damage was caused by rarefaction, but this is partly because most fixtures are more sensitive to rarefaction than to compression. Roller-type doors were consistently pushed inwards, which would have required a compression phase of around 50 mbar. The largest rarefaction damage corresponded to an underpressure of at least 75 mbar. It can be expected that the compression phase was of larger amplitude and shorter duration than the rarefaction phase, but there were few fixtures sensitive to compression, so the real level of compression was never seen.

A reasonable estimate is that the site was exposed to a patchy blast wave consisting, at the fence, of up to 40 mbar overpressure followed by 40 mbar underpressure, with ground effects and acoustic reflection meaning that some targets experienced twice this. The decay of the pressure wave across the site was rather slow, with buildings several hundred metres from the site edge experiencing significant damage.

It should be noted that pressure is expected to decay inversely with distance in the far-field from a long duration event. It should also be noted that the areas (pressure multiplied by duration) of the compression and rarefaction parts of the wave are expected to be equal. In general, the compression phase is of a larger magnitude, and of shorter duration.

2.5 Time duration of blast wave

We have a variety of reasons for asserting that this was a long time duration event.

2.5.1 Comparison of near and far-field damage

The survival of an unprotected brick wall 10 m from the explosion centre, compared to the level of far-field damage, also implies a very slow event. The brick wall at point 3 on the Fig. 1 was cracked, but not fully pushed over. This wall would not have been able to withstand a pressure differential across it much in excess of 50 mbar. However, if we naively assume a spherical decay to a pressure of around 50 mbar 150 m away (at point 10 on Fig. 1), this would imply a pressure of 750 mbar or more at the site of the wall.

This assumption is obviously crude, since some of the blast may have been generated more than 10 m from the centre of the explosion, and also because the damage at a greater distance was fairly directional. None the less, if we take a reduced figure of, say, 400 mbar for the pressure at 10 m, take the wall size at 2 m, and take the pressure wave as travelling outwards at the speed of sound, then we reach an estimate of at least 50 ms for the rise time of the event. This implies hundreds of milliseconds for the duration of the whole event.

2.5.2 Comparison of near and far-field damage

A figure of hundreds of milliseconds for the time duration of the event is also supported by similar comparisons between the near and far-field damage levels which are shown in Fig. 2. For an inefficient non-shocked pressure wave of time duration T, pressure is expected to decay inversely with distance when the distance from the explosion is much more than cT (in accordance with acoustic theory), where c is the speed of sound. Here, pressure does not decay inversely with distance until hundreds of metres from the event. This suggests a time duration of hundreds of milliseconds.

2.5.3 Materials and Transport building

The nature of the damage to the Materials and Transport building (see Appendix B) gives an estimate for the duration of the rarefaction pulse or more than 100 ms. This indicates that the blast-generating event had a long duration.

2.5.4 A&I warehouse

The damage of the A&I warehouse also indicates quite a long duration event, since the damage on the sheltered side of the building is similar to that on the nearside. (When the wavelength of a pressure pulse is much less than that of building, acoustic reflection gives much worse damage on the nearside.) The similarity in damage between the sides means that the pressure wavelength was at least of the order of the size of the building, which again indicates an event of more than 100 ms.

2.5.5 Failure mode of vessel

Brittle cracks branch at propagation velocities above about $0.2c$, where c is the speed of sound in the material [4]. The speed of sound in steel is 5180 m/s. There was no significant branching in the failure of the vessel, so if the cracking were brittle it must have been going at 1000 m/s or less. A ductile crack would be even slower.

The fastest that a crack could propagate without branching around the 7 m circumference of the vessel is about 7 ms. The rupturing event must have taken longer than this, which is consistent with a pressurised vessel failure, but would not be consistent with a detonation for example (even a slow detonation). This lower bound on the time duration of energy release is mainly of use for ruling out the possibility of a "soft" liquid phase detonation.

2.5.6 Missile 47

Missile 47 was flung 75 m. We can calculate a minimum time for this missile to receive sufficient impulse, given that it did not receive a sufficiently great force to break the box cover.

As stated, Missile 47 was flung 75 m. This implies that it had an initial velocity of at least 55 m/s. Since the missile weighed 12 kg, we can infer that it received an impulse, I, of at least 660 kg m/s. First, we calculate whether the light cover would have responded dynamically or quasistatically to the pressure wave. The cover of the missile had an area density, D, of around 3.3 kg/m^2. The projected area, A, which the missile would have offered to an explosion would have been between 0.3 m^2 and 0.03 m^2 depending on the orientation. We taken an estimated area of 0.1 m^2. In reality, some counteracting impulse would also have been received by the opposite face of the fitting, which means that the impulse received by the face has been underestimated. If the missile received such an impulse over a time T seconds, then, if the cover responded to the impulse dynamically, it must have been displaced by a distance of

$$0.5IT^2/(DA) \approx 1000\ T^2 \text{ m}$$

The area density of (either half of) the cover was around a tenth of the area density of the light fitting itself, which implies that that this displacement must have been almost entirely relative to the fitting. Examination of the fitting allows us to conclude that 10 mm displacement of the cover relative to the fitting would have been up upper bound. Dynamic response is therefore only possible if $T < 3$ ms.

We have good grounds for believing that the time duration was at least 3 ms, for example, from the vessel failure. This is also implied by the intact glass tube in the light fitting. We therefore conclude that the light box cover was subjected to a fairly static load.

We can also relate the maximum static loading experienced by the cover to the impulse received:

$$T = I/(P_{\max} A)$$

Whatever the orientation of the light fitting, the front (translucent) cover would have been subjected to a pressure close to the peak pressure.

We have tried static loading (weighting) an identical light box to find out at approximately what pressure the front cover would have failed. Throughout the testing, we tried to ensure that the test procedure would given an upper bound on the failure pressure.

A 30 cm section from the centre of the light was tested. The curved end of the light would have given a little additional strength to the light, but, as the aspect ratio of the light was more than 10:1, the additional strength would have been slight.

Under uniform pressure loading, the failure mode would have been breaking

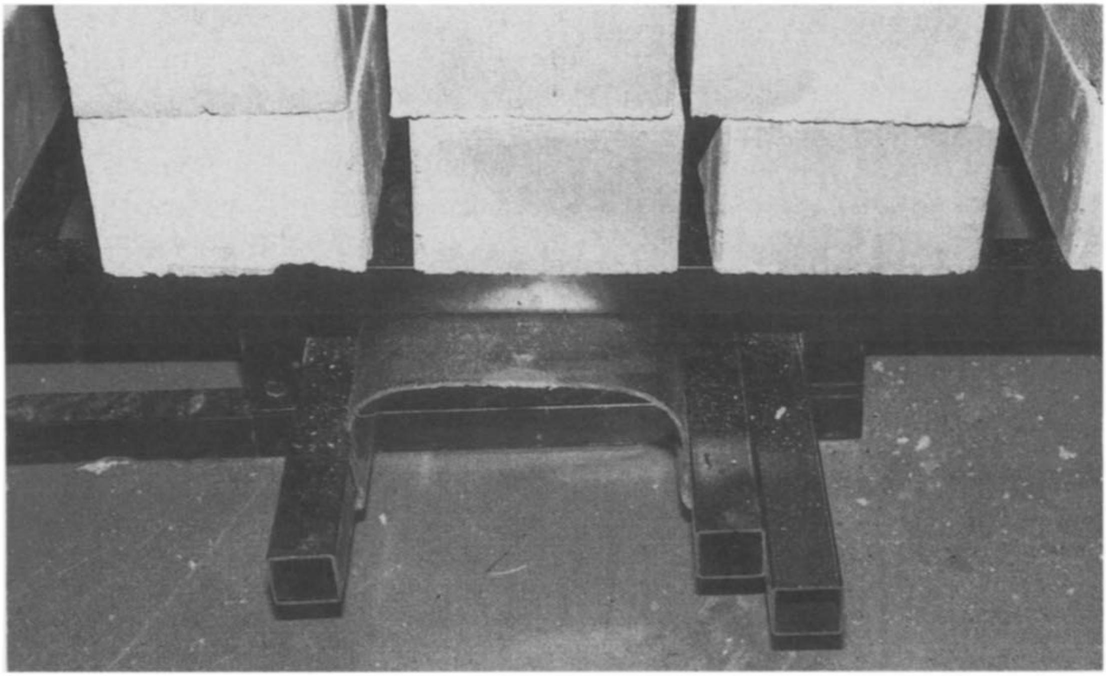

Plate 3. Light box loading.

along the maximum radius of curvature. Uneven loading would have resulted in failure at a lower average pressure. To ensure that the failure mode in the loading test was the same as it would be from a pressure wave, we clamped the edges of a section of cover, to prevent it splaying sideways (Plate 3).

The top face of the section was then steadily loaded until it failed. When it failed, it started by cracking along the line of maximum curvature, and then shattered. It failed at a loading of 3920 N. The area of the top of the section was 0.036 m^2. This corresponds to a pressure of about 1.1 bar.

From these estimates, we can conclude with confidence that the light fitting could not possibly have been exposed to a pressure of more than 2 bar, and that the pressure was probably a deal less than this. The light fitting would also have been weakened by a flame before surviving blast.

This is important for two reasons: first because it implies that the time duration of the pressure wave close to the vessel was at least 30 ms (to get sufficient impulse, taking a projected area of 0.1 m^2), and secondly because it implies that blast was generated further away from the vessel than where the light fitting was.

Straightforward expansion of a pressure wave which started from a 1 bar source with a radius of a couple of metres could not have yielded 500 MJ without an additional source of energy. The maximum blast energy (based on an ideal gas calculation) [5] from the adiabatic expansion of a gas is around:

$$P_s \cdot V[1-(P_s/P_a)^{(1-\gamma)/\gamma}]/(\gamma-1)$$

where P_s is the source pressure, P_a is atmospheric pressure, V is the source volume, and γ is the ratio of specific heats.

If we take a source pressure of 2 bar (i.e. 1 bar overpressure), and a radius of 3 m (which is an estimate of the distance between the vessel centre and the light), the available energy is 11 MJ, which is completely inadequate. After vessel failure, the contents of the vessel would expand very roughly uniformly, since they would be nucleating and forming a droplet cloud rapidly after depressurisation. This means that any subsequent release of energy, after the contents had expanded to a radius of around 3 m (which is what would be expected from a more continous release of energy from within 3 m), would also imply that most of the energy was released from outside a radius of 3 m.

This leads to an important conclusion, namely, that most of the damaging blast originated more than 3 m from the reactor vessel.

3. Other evidence on the incident

Several other pieces of evidence are important in determining the nature of the blast-generating event in the explosion.

3.1 Originating event

The pressure and temperature read-outs from the reactor vessel in Appendix E, clearly show that in the run up to the explosion, this vessel became heated and pressurised. A comparison of the temperature/pressure relationship with that expected for the vessel contents showed a far higher than expected pressure, indicating that there was probably some unknown gas being evolved within the vessel. At the process temperature of 165°C a pressure of 0.2 bar was expected, whereas the readings show around five times this.

It is unlikely that the vessel was being heated externally (e.g. by a jet fire impingement) since the vessel had a pressurised water jacket, which showed no signs of being heated and would have prevented heat flux through the sides. In addition, external heating would probably have been noticed by the operators (one of whom was on the plant structure at the time). There are signs from the read-out that the reaction started going "wrong" (shown by unexpectedly high pressure) some 35 minutes before the temperature started to rise rapidly. The water jacket was switched to cooling when the temperature in the vessel approached the intended process temperature.

It seems most likely from the evidence that the indicating event was a runaway reaction within the vessel. The possible causes of the runaway are being reported upon elsewhere [2]. The only conclusion relevant to the present discussion is that the most likely runaway mechanism involves the evolution of ketene.

3.2 Fire damage to missile 47

A study of missile 47 gives important information about the sequence of events in the incident. This missile landed 75 m from the explosion centre, and had been significantly burnt prior to being projected.

Having tested similar light fittings at Thornton Research Centre (Appendix F), we conclude that this light fitting had been burnt by direct impingement of a jet fire, rather than by radiation. The jet fire impinged the light fitting end-on. Both the front cover and the back face of the light fitting had been impinged. The jet fire had lasted between 30 seconds and 2 minutes before the explosion took place.

The damage to this light fitting (Plate 2A) was very similar to that on an identical light following exposure to a 0.7 m sooty, diffusive acetylene flame for 25 s (Plate 2B). The acetylene flame was relatively fierce (with a conductive heat flux of around 150 kW/m^2) compared to what is likely to have occurred above the vessel. So it is fairly safe to conclude that the light fitting had been exposed to a jet fire for at least 30 s, and at most for two minutes.

The form of damage on Missile 47 is much closer to that expected from a small high-speed jet flame than from a larger meandering flame, since the damaged area has a very clear boundary in two directions.

The jet was almost certainly from a flange failure above the vessel or from an opening crack above the vessel, rather than from the end of the safety valve duct. The safety valve duct ran to above the roof, where there were no lights. There were several lights above the vessel itself, and it seems very likely that Missile 47 was one of those.

The results of this test are important for three reasons: first, they establish that there was a jet fire from a flange failure before the explosion took place, for at least 40 s. This gives an indication of the rate of runaway, and also means that we can conclude that there was already a large source of ignition when the vessel ruptured. Second, they establish that there was missile-generating blast well away from the vessel (that is, missiles were generated by blast: from things that were not vessel fragments, nor in contact with vessel fragments, rather than by impact by vessel fragments). An end-on light fitting is rather streamlined, and the blast wind from the explosion must have been very considerable to blow it 75 m, particularly as the event had a long time duration. Thirdly, we can infer that one of the gases produced in the runaway reaction was flammable. This fits with a suggested mechanism for the runaway involving ketene.

3.3 Eye-witness reports

There are eye-witness reports to support the sequence of events described in the conclusions. In particular, there is a report of flames from above the vessel before the vessel rupture, and of a large fireball.

4. Calculations on explosion scenarios

It seems most appropriate to start this discussion of the blast pattern with some calculations on what the damage pattern would have been from various possible incidents.

4.1 Blast from a vessel rupture

Pressure release from normal pressurised rupture of liquid above its boiling point depends on the percentage of the liquid that immediately vaporises on depressurisation. For relatively small percentages (for example, typical propane BLEVEs, where the percentage is around 20%) only the vapour above the liquid gives significant blast.

When only a small percentage of the liquid is evolved as vapour, the rate of evolution of vapour is small, since it is limited by heat conduction (rapid boiling, which gives rise to vapour and condensate, requires a heat transfer from droplets to the gaseous phase). In this case the liquid phase does not contribute significantly to the blast.

For larger percentages (above an unknown critical value, but probably near 100%), presumably the liquid phase vaporises fast enough to contribute to the blast. Such a possibility would be unusual, but it is worth considering in view of the unusual level of blast.

We first estimate the blast energy by assuming that we are below this critical value. As a guideline, if we take 3 m^3 of vapour phase released at 80 bar, then the equation used in Section 2.5 gives 44 MJ. This is inconsistent with the level of blast. The energy yield was well over ten times, and probably hundreds of times, larger than this.

The far-field damage (at Thornton Research Centre, see Section 2.4) allows us to bound the energy yield below with a figure of 500 MJ (although this figure was from a single door bolt, it is consistent with the damage throughout Thornton) and estimate a figure of at least 25 000 MJ released at source. A vessel rupture with 3 m^3 of vapour would have to be at around 800 bar (which gives 520 MJ) to give the smaller of these figures. This pressure is totally impossible from the kind of vessel, and inconsistent with the near-field damage. An energy yield close to the higher figure would be orders of magnitude beyond what could be accounted for.

The possibility that the liquid phase might contributes should be considered. For the release of a pressurised vessel containing a single liquid or solution, this is possible. For example, if a pressurised vessel of pure DMAC were heated until it reached 70 bar, this would be likely.

As a rough calculation, liquid DMAC has a specific heat capacity of around 2 kJ/kg K. For pure DMAC to have a vapour pressure of 70 bar, it would have to be at a temperature of around 700 K. (Manufacturers' data stops at 60 bar, 670 K.) The latent heat of vaporisation of pure DMAC is around 500 kJ/kg.

The excess stored thermal energy above boiling point at 70 bar is therefore around 540 kJ/kg. This is above the latent heat of vaporisation. The evolution of vapour from 70 bar DMAC in liquid phase would not be time-limited by heat conduction (for the release of a superheated liquid there is usually a rate limit associated with the required heat transfer from the liquid to the interface near nucleation sites).

The intended vessel contents were, of course, a rather concentrated solution, and would have had thermodynamic properties quite different from those of pure DMAC. Specifically, the contents would have a higher latent heat of vaporisation, and the vapour pressure also would be lower at a given temperature.

However, it is clear from the pressure/temperature trace for the vessel before rupture that some other vapour/gas was being evolved in (or was leaking into) the vessel. The presence of a jet fire and evidence that the runaway reaction evolved ketene confirm the belief that a gas was being evolved. The evolution of vapour by the runaway would greatly lower the temperature at which the failure pressure of the vessel was achieved.

Once the temperature of the vessel reached around 230 °C, the DCNB/DMAC mixtures in it would start to decompose [2]. This would also involve the evolution of gases.

Although it is impossible to perform detailed calculations on the (unknown) chemicals in the vessel at the time of failure, the presence of significant quantities of evolved gas makes it very unlikely that the temperature would have been high enough at vessel rupture to give liquid phase contribution to blast.

4.2 Missiles from a vessel rupture

Calculating drive pressures from missiles is notoriously unreliable, and always underestimates the drive pressures. Typically, pressure calculated on the basis of a naive missile model is, at most, 20% of the actual rupture pressure [6]. More sophisticated theoretical missile models have been developed recently [7], but have not yet been verified, and calculations are dominated by thermodynamic and statistical uncertainties. We will therefore analyse missiles on the basis of an empirical model.

As a very rough guide, a missile such as Missile 28, which travelled about 500 m, must have been travelling at at least 70 m/s (which assumes a 45° initial flight angle), and has an area density of about 500 kg/m^2. According to the (experimentally derived) guidelines in [8], the upper velocity limit for a fragment from a ruptured vessel is roughly

$$v = 0.88\, c\, (PR/mc^2)^{0.55}$$

in terms of the rupture pressure, P; the vessel radius, R; the area density of the projectile, m; and the speed of sound, c.

If Missile 28 were a vessel fragment, it would therefore correspond to a drive pressure of at least 40 bar. The missile was not a vessel fragment but a nozzle, and therefore we can infer that the pressure that it experienced was in excess of this. All that this does is show that there is no definite inconsistency between the missile distances and the claim that missiles originated from a 60–80 bar vessel rupture.

None the less, the number of missiles was very high, and calculations based on Missile 47 indicate that the missile-generating blast had a long duration. It is likely that the number of missiles was considerably increased by blast wind from an ongoing explosion.

4.3 Non-combustive contributions to blast

At some point during the course of the vessel failure, and subsequent depressurisation and dispersion of the reactor contents, the chemical evolution of energy would cease. Although the initial stage of the runaway reaction was complicated, it is likely that the final stages involved straightforward thermal decomposition of nitro-compounds.

It is clear that, since the calculation in Section 4.1 naively assumed that the evolution of chemical energy ceased immediately when the pressure reached the failure pressure of the vessel, it neglects any contribution from the chemistry after vessel failure. An extreme case where this calculation would be in error is that of a liquid phase detonation, where the bulk of the chemical energy would be released before dispersion could take place.

In the present case, there is no doubt that the blast from a simple vessel rupture could have been considerably enhanced by the decomposition running on during the dispersion of the vessel contents. It is, however, very unlikely that chemical run-on alone was the major cause of blast.

The first reason for asserting this is the duration of the blast-generating event. The blast wave had a duration of hundreds of milliseconds. This implies that the blast-generating event must have pushed the surrounding air (like a spherical piston stroke) for this order of time duration. During a hundred milliseconds, the event itself must have expanded to a radius of tens of metres (since it would have been expanding at close to the speed of sound). During such an expansion, a considerable amount of air would have been entrained.

It seems unlikely that non-combustive chemistry which was slow enough to be relieved by a vessel failure over perhaps 10 ms (in the sense that it did not force the vessel to fail faster) would have maintained its heat release rate after it had been dispersed over thousands of cubic metres, and been cooled by entrained air.

In addition, we conclude in Section 2.4 that the energy released at source was probably well in excess of 25 000 MJ, which is more than could be generated by non-combustive chemistry, even if *all* of the available non-combustive energy had been released.

Based on vessel contents of 4 tonnes DCNB/DFNB and 6 tonnes of DMAC, the decomposition energy available (see Appendix G) was about 8000 MJ.

4.4 Combustive contribution to blast-generation

In a sense, the distinction between non-combustive and combustive contributions to the blast is a little blurred, since it is unlikely (even without a strong ignition source) that air would not have become involved in the chemistry during this process.

There was a strong ignition source outside the vessel. Ketene (which is highly flammable) was indicated as present. The bulk contents of the vessel were also flammable (at their release temperature, although not at room temperature: DMAC has a flash point of 70 °C), and the runaway reaction may have resulted in a whole range of chemical intermediates being vaporised also.

It is therefore most likely that the rupture would result in a sudden high-speed jet release of about 10 tonnes of highly flammable material from a source pressure of perhaps 70 bar, with an energetic ignition source. It is also quite possible that the whole mixture would autoignite when exposed to air, even without an ignition source.

Such a phenomenon is already a little beyond anything that has been tested experimentally, and is further complicated by a proportion (perhaps most) of this release being into a very highly congested area. High levels of congestion can greatly increase the severity of diffusion limited processes (such as vapour cloud explosions), since the congestion generates high levels of turbulence, which increase the mixing rate. This resulting combustive event is the most likely source of most of the blast observed. The fact that such an event would be rate-limited by air mixing into the fireball (albeit at a very high level of turbulence) would make such an event of long duration compared to a vapour cloud explosion (which is limited only by the diffusion of heat and radicals away from the flame-front).

The typical duration of a vapour cloud explosion is perhaps 50 ms. An unconfined fireball from a low-pressure source can last for 10 s. It is easy to see that a high-speed congested fireball might last for, perhaps, 400 ms.

The combustive energy available was around 230 000 MJ (based on 4 tonnes of DCNB/DFNB with a heat of combustion of 14.5 MJ/kg, as in Appendix G, and 6 tonnes of DMAC with a heat of combustion of 29 MJ/kg). By comparing these figures with estimates in Section 2.4, we can see that a combustive event involving about a fifth of the vessel contents in the congested region would explain the blast well.

5. Probable sequence of events

The most likely description of events from our investigation is as follows:

(1) There was a runaway reaction in the reactor vessel, evolving some gas (almost certainly ketene and carbon dioxide [2]), which caused the pressure to rise rapidly once the vessel approached its process temperature.

(2) As the pressure rose, the safety valve blew. A flange (or similiar) failed

above the vessel and gave rise to a jet fire. The jet fire carried on burning for at least 30 s before vessel failure.

(3) The vessel burst, at a pressure of around 60–80 bar. The vessel tore into two major and several minor fragments. The vessel fragments, and many surrounding pieces of plantwork, were turned into energetic missiles, which flew up to 500 m away. The contents of the vessel did not detonate.

(4) As the vessel failed, the vessel contents continued to release energy, entrained air and rapidly ignited. The entrainment of air and combustion were greatly speeded up by the highly congested environment in which the vessel failure took place. The blast wind from this combustive event probably increased the number and severity of the missiles.

(5) A large fireball extending outside the structure occurred. A secondary fire started, which quickly involved the inventory of some nearby xylene storage vessels.

We summarise the reasoning behind each of the steps above.

(1) The event seems to have started inside the vessel. This is clearly indicated by the pressure/temperature plot of the vessel (Appendix E). External heating is very unlikely not to have been noticed by the operators on the timescale concerned, and would have affected the water jacket temperatures. Some evolved gas is also shown up by the vessel data, which indicate that the event started inside the vessel. This view is supported by an investigation into the runaway processes reported on elsewhere [2].

(2) Eyewitnesses report the safety valve lifting significantly before the vessel exploded. The valve itself was ducted to outside the plant structure, and could not have been the source of the jet fire which burned Missile 47. There was therefore another leak in the vicinity of the reactor vessel (where there were light fittings). The jet fire lasted at least 30 s before the missile was blown away from the fire, since the fire damage on Missile 47 could not have been achieved in less than this.

(3) Detonation can be ruled out by the small number of large vessel fragments. The pressure in the vessel was adequately relieved on the timescale of the crack propagation, which was several milliseconds. The number of missiles was remarkably high, but not conclusively inconsistent with being from a vessel rupture.

(4) The time duration of the blast wave implies that energy continued to be released well after the vessel had ruptured. The amount of energy released into the far-field also implies energy release after the vessel had ruptured. Since the contents were rapidly expanding, this implies energy released when the contents occupied a large volume, when air would have been entrained. There was an energetic ignition source and, without combustion, it is hard to account for the total energy yield. The vessel was underneath a concrete floor, and surrounded by very congested structure, so that

for any burst point part of the contents are bound to have been expelled at high speed into a congested geometry. A highly congested jet fireball seems inevitable, and could account for the high level of damage.

(5) The fireball and xylene fire were well documented.

6. Conclusions

The CFA explosion was initiated by a runaway reaction in a reactor vessel. Before the reactor vessel failed, there was a jet fire outside the vessel for around a minute.

The main reason for the very high level of blast was that the vessel contents were released at very high speed and ignited in a very congested area. The major blast generating event was a *highly congested jet fireball.*

The blast wind from this fireball was partly responsible for the high number of missiles.

Acknowledgements

An investigation of this kind could never be the work of a single individual, and the author acknowledges the support of many others, particularly David Bull, Richard Tucker, Bernard Samuels and Terry Cotgreave in various parts of this paper. The cooperation and assistance of the management at Shell Stanlow Manufacturing Complex is also gratefully acknowlegded.

References

1 Overpressure Monograph: First Paper of the Major Hazards Assessment Panel, Overpressure Working Party, Institute of Chemical Engineers, London, 1989.
2 F. Bodurtha (Ed.), Industrial Explosion Prevention. McGraw-Hill, New York, NY.
3 B.R. Lawn and T.R. Wilshaw (Eds.), Fracture of Brittle Solids, Cambridge University Press, Cambridge, 1975.
4 M.R. Baum, Disruptive failure of pressure vessels, Presented at the 1987 Pressure Vessels and Piping Conference, San Diego. CA, 1987.
5 B.E. Gel'fand, S.M. Frolov and A.M. Bartenev, Calculation of the Rupture of a High-Pressure Reactor Vessel, Trans. Fizika Goreniya i Vzryva, 24 (4) 114–123.
6 M.R. Baum, The velocity of missiles generated by the disintegration of gas-pressurized vessels and pipes, J. Pressure Vessel Technol., 1106 (1984) 362–368.
7 D.R. Stull, E.F. Westrum and G.C. Sinke (Eds.), The Chemical Thermodynamics of Organic Compounds, Kreiger, Malabar, FL, 1987.
8 S.W. Benson (Ed.), Thermochemical Kinetics, Wiley, New York, NY, 1968.
9 Kirk-Othmer Encyclopaedia of Chemical Technology, 3rd edn., Wiley, New York, NY, 1986.

Appendix A

The location of missiles is marked on the map in Fig. 3. There follows a brief description of each missile. The masses of most missiles were directly measured. Those estimated are marked with an asterisk (*).

No.	Description	Mass (kg)	No.	Description	Mass (kg)
1.	Instrument	0.75	37.	Pipe debris	?
2.	Pipe	*70	38.	Pipe debris	?
	Handrail	4	39.	Plate debris	?
	Flange	6	40.	Plate debris	?
3.	Vessel nozzle	56	41.	Cable tray	*7
4.	Instrument head	1	42.	Plate	<0.5
5.	Instrument base	13	43.	Reactor foot	71
6.	Instrument valve	<0.5	44.	Reactor foot packer	89
7.	Unistrut	5	45.	2 m pipe	37
	Instrument coupling	4		Pipe and flanges	38
	Handrail	*2-3	46.	Reactor foot packer	88
8.	Casing fragment	0.75	47.	Light box	12
9.	Casing fragment	0.75	48.	2 m pipe	26
10.	Casing fragment	0.5	49.	Unistrut	*3
11.	Casing fragment	0.5		Instrument probe	*3
12.	Casing fragment	1		DP cell	*3
13.	Instrument	1.5	50.	Valve yoke	*2
14.	Casing fragment	<0.5	51.	2 m pipe	*35
15.	Debris		52.	Cock	*25
16.	Pipe	4	53.	Pipe	*75
	Debris		54.	Floor grating	*45
17.	Pipe	7	55.	Valve bonnet	15
18.	Pair of flanges	15	56.	Floor grating	6
19.	Dead end lubricator +	10	57.	Vessel	probably >1000
20.	Pipe	*70	58.	Flange	<0.5
21.	Valve actuator	70	59.	Lagging sheet	<0.5
22.	Ball valve	46	60.	Handrail	3
23.	Vessel fragment	*15		Pipe	*7
24.	Control valve fragment	3	61.	Cable tray	5
25.	Instrument stand	21	62.	Probe	38
26.	Cable tray	5.5	63.	Instrument	<0.5
	Debris		64.	Pipe fragment	<0.5
27.	Cock and flange	7	65.	Nipple	<0.5
28.	Vessel nozzle	51	66.	Instrument	6.5
29.	Reactor top fragment	675	67.	Gear box support	35
30.	Instrument level cock	<0.5	68.	Reactor drive coupling	137
31.	Flanges	2.5	69.	Debris	*3
32.	Seal cartridge (reactor)		70.	Debris	*3
33.	Instrument stand	21	71.	Floor grating	60
34.	Gear box (reactor)	365	72.	Lamp fragment	<0.5
35.	Pipe debris	(35–38 total	73.	Instrument	4.5
36.	Pipe debris	about 25 kg)	74.	Plate	*7
			75.	Reactor shell fragment	*150

Appendix B

Inspection of Stanlow site damage

Numbers refer to the number in Fig. 1.

(1) The structure around R7601 (the reactor vessel) had been devastated. I was not able to identify very much within a couple of metres of it. The damage extended some distance back into the structure, although the far side of the plant was hardly damaged at all. Even though the vessel split was along an outward face of the vessel, the bulk of the vessel ended up outside the structure. A lot of the devastation of the plant appeared to be associated with the failure of the north-west leg of the concrete roof over the vessel. The roof is clearly identifiable. Most of the visible damage was ductile rather than brittle, although this is probably because most of the structure was metal (distance from explosion centre 0–5 m). Plate 1

(2) Small one-storey brick building was completely deroofed. There was slight damage to the top couple of courses of bricks. No damage was detectable further down the wall. The roof was of corrugated construction. The bottom part of this building was well shielded from the blast. The pressure differential across the walls would have been relieved by the failure of the roof. The damage of the top was similar to the damage that would have been caused by a TNT blast wave of overpressure 150 mbar (distance from explosion centre 35 m).

(3) Single-storey control room was badly damaged structurally, but left standing. The nearest corner on this steel-framed building was debricked and deroofed, leaving only the steel frame with a little structure leaning against it. Half-way along the nearside, at about 15 m from the explosion centre, the wall was intact with only the roof missing. This indicates either quite a rapid decay in shock strength, or very directional damage (more probably the latter). From standard TNT tables [1] the damage to the near corner is similar to the damage that would have been caused by a TNT blast wave of overpressure 500 mbar shock wave, whereas the damage half-way along the wall could correspond to nearer 150 mbar.

The far side of the control room was intact (in the sense that the far wall is largely undamaged), but it had clearly been sheltered from the blast by the rest of the building. There is a strong tendency towards increasing damage with height. A first-floor brick wall (some sort of staircase?) towards the back of the control room has been moved and broken, at a distance of around 25 m from the explosion centre (distance from explosion centre 10–25 m).

(4) A single-storey steel-framed decontamination building close to the explosion centre had been completely gutted. The steel frame was bent, but probably by missiles rather than blast (a flight of stairs seems to have landed on this building). The damage to this building was similar to the

damage that would have been caused by a TNT blast wave of overpressure about 500 mbar (distance from explosion centre 15–20 m).

(5) A single-storey steel-framed corrugated sheet building had all of the sheeting ripped away on the front and back faces. A large tank had been shifted along the ground towards it. The damage to this structure probably is similar to the damage that would have been caused by a TNT blast wave of overpressure 400 mbar (distance from explosion centre: 15–20 m).

(6) Nearby (single-storey) control room mainly intact. A one-brick (9″) wall moved about 0.5 m. One window and frame bent inwards. Closest window to explosion virtually unaffected (3 of 16 panels broken). Wall movement was outwards. This is similar to the damage that would have been caused by a TNT blast wave of underpressure 200 mbar (distance from explosion centre: 30–40 m).

(7) Amenity block. This temporary block was of a wooden-framed construction and was two stories high. The end wall of this building, facing towards the explosion centre, was caved inwards, but the rest of the upper storey walls were sucked outwards. The side facing the building was sucked out much more violently than the far side, with the panel wall being nearly a metre displaced at the top. The design of such buildings is such that they are much more sensitive to rarefaction than compression, but the damage to this building probably corresponds to 150 mbar of rarefaction and compression on the sides facing the explosion centre. The building was shielded from direct line of sight from the vessel (distance to explosion centre: 40–55 m).

(8) One wall on the sulfolane plant facing towards the explosion centre had been sucked outwards. An L-shaped beam had been bent outwards and the corrugated sheeting attached to it was buckled. The sheeting had not torn much, with only two of the screws attaching the sheeting in place ripped out. Some calculations on this beam are included in Appendix C. The conclusion is that the wall was subjected to an underpressure of around 180–220 mbar (including the strength of the sheeting itself) (distance to explosion centre: 65 m).

(9) The corrugated sheeting on this warehouse was "rippled" throughout. Interior (unattached) support struts had been bent inwards, and the sheet was left bent outwards. This allowed the figures for both the compression and rarefaction part of the pulse to be estimated. The manufacturers provided the information that the sheeting (with this span) would move 2 cm elastically, if subjected to around 25 mbar, but in this case the deflections were far greater, so we performed some testing on the sheeting ourselves. The conclusion was that at an overpressure of around 30 mbar the sheeting yielded completely. The deflection of the sheeting in this regime therefore gives only an indication of the energy in the overpressure and underpressure.

Interestingly, the damage to the different sides of the building was very similar. The whole building was sheltered from direct blast, but even so the wavelength of the pressure disturbance must have been comparable to the size of the building to give similar damage to the different sides. The largest deflections measured in the sheeting were on the far side on the building from the explosion, and next to the doorway. Allowing for the structural members that also bent in the explosion gives a lower bound of 45 mbar for the overpressure, and 25 mbar for the underpressure. The degree of deflection gave a minimum figure of around 600 J/m^2 for the energy density of the compression phase, and about half that for the rarefaction phase. The degree of shelter that this building had, together with the very long duration of the pulse experienced, means that this would give an underestimate of the yield of the explosion (distance from explosion centre: 90–115 m).

(10) The materials and transport building suffered a lot of window damage, with some slight damage to corrugated sheeting (not counting missile damage). The windows facing towards the explosion centre were all pulled outwards, some completely out of their frames, others just broken and bent. The windows were wire-reinforced glass. On the far side of the building some of the windows were slightly pushed inwards, but none were sucked outwards.

The most likely intepretation for this pattern is the following sequence of events. The building was first subjected to a compression wave, which buckled many of the windows inwards, on both sides of the building. The building was not air-tight, and there would have been some air let in around the buckling, but even so, the corrugated sheeting had not failed much, which means that this overpressure cannot have been much over 50 mbar. (The span between vertical bolts on the corrugations was 120 cm, the figures supplied by the manufacturers of similar sheeting suggest that this would have failed inwards at around 70 mbar). This was followed by a rarefaction wave, which sucked many of the front windows out completely. However, once these windows had been sucked out, the pressure inside the building fell rapidly enough to prevent suction damage on the rear-facing windows. The venting of the building during the rarefaction makes it hard to quantify the level of rarefaction pulse, but probably it was also around 50–100 mbar (distance from explosion centre: 150–170 m). See Plate 4.

If we accept this sequence of events, we can estimate the time duration of the rarefaction pulse. A large sharp-edged hole with a drive pressure of 5 mbar vents air at about 30 m/s. If we take 50% of the windows as venting, the building has roughly 1 m^2 of vent per 200 m^3 of building volume. The timescale over which pressure would vent is therefore around 30 mbar. The duration of the rarefaction pulse was therefore probably at least 100 ms (since it has to have a rise time of about 30 ms). This suggests again that the pressure rise and fall was relatively slow, corresponding to a long event. It is remarkable that com-

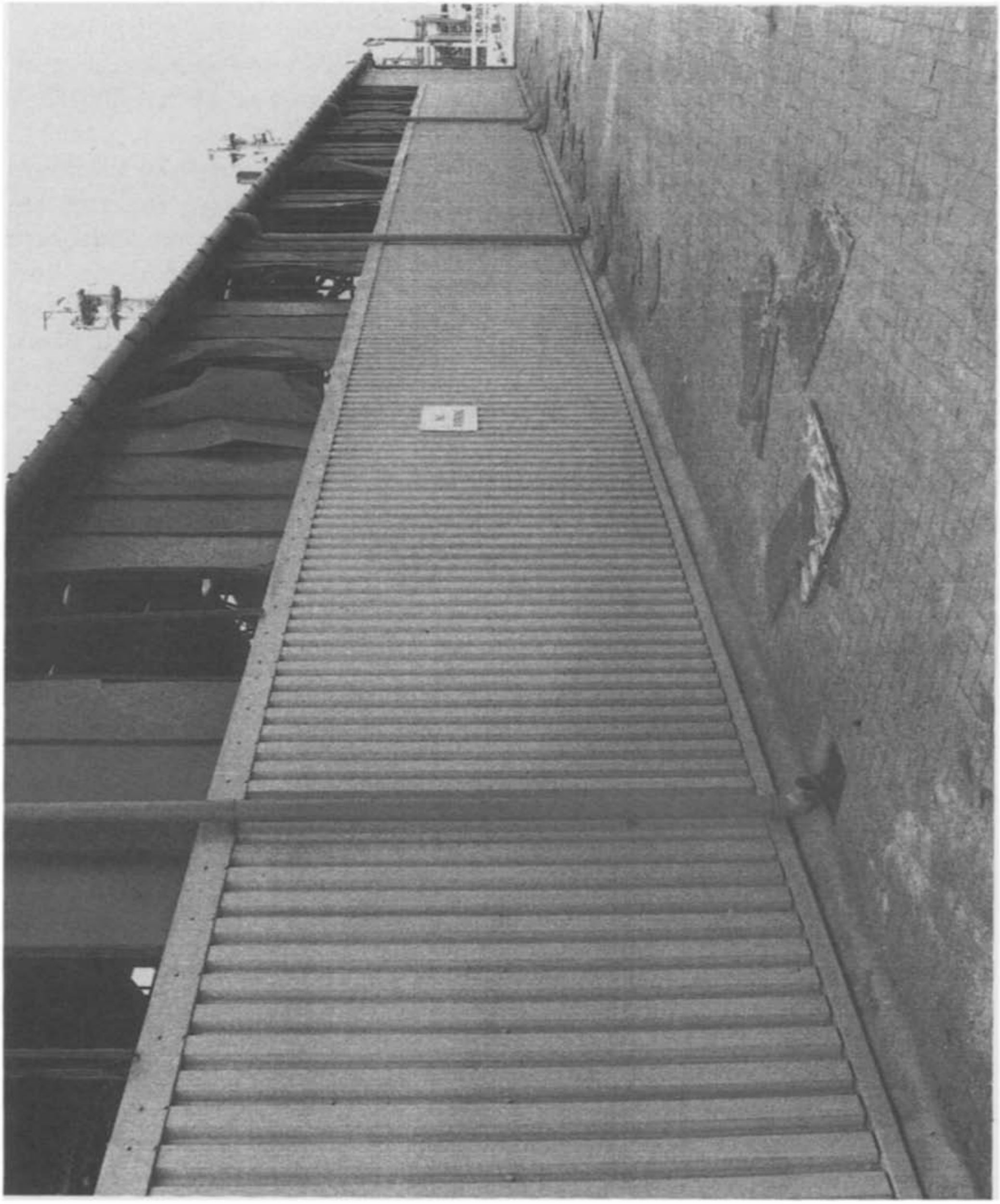

Plate 4. Damage to materials and transport building 150 m from explosion centre.

parable damage, although slightly milder (the frames moved, but no windows fell out), to this occurred to the wire-framed windows of Building 58 on the Thornton site, at a distance of 460 m from the explosion site.

(11) A high plant building was completely deroofed. The roof was a brittle corrugated sheet, which would have broken up fairly easily. The damage may have been caused by as little as 20–30 mbar, but it is impossible quantify accurately (distance from explosion centre: 35–60 m).

(12) The corrugated sheets on the roof of this substation were very slightly rippled. The overpressure required to do this was only 30 mbar. (distance from explosion centre: 70 m).

(13) Three walls of this corrugated sheet but were rippled and left been outwards. The underpressure required to do this was around 30 mbar (distance from explosion centre: 40 m).

(14) The building behind the xylene storage area was probably mainly affected by fire damage. The window frame on the near side to the explosion was presumably pushed inwards by the explosion, which would have required an overpressure of perhaps 100 mbar. The damage to this window suggests that the Keebush xylene vessels may have started leaking due to the blast damage, rather than the subsequent fire (distance from explosion centre: 40 m).

(15) One window frame on the alcohols PU workshop, facing towards the explosion, was sucked out by a few centimetres. This would require a static pressure more than 50 mbar. There was slight wall movement in this building, which again suggests that the underpressure felt here was perhaps 100 mbar. Since this building is adjoining the materials store, they probably experienced similar pressures. (There are no nearby buildings to reflect or shield pressure.) This therefore lends weight to a figure of 100 mbar rarefaction for the materials building, with damage mitigated by venting through the windows which came out, and supports the claim that the pressure pulse was long in duration (distance from explosion centre: 160 m).

(16) A 4 m high corrugated sheet building away from the main blast direction was pushed in at the top, and was bulged at the bottom. This indicates that at this location the compression was definitely stronger than the subsequent rarefaction phase (distance from explosion centre: 25 m).

(17) The corrugated roof of this building was slightly bent outwards (distance from explosion centre: 80 m).

(18) This building had slight ripples in the corrugations (distance from explosion centre: 80 m).

Appendix C

Structural calculations

This appendix collects together calculations of the internal pressure required to rupture the fluoroaromatics reactor vessel and propagate cracks in the vessel wall, and the external pressures to cause damage observed on other objects in the far field. In all cases the calculations are quasistatic. The greatest sources of uncertainty concern the properties of the materials in question.

C1 Rupture of reaction vessel by internal pressure

C1.1 Rupture of vessel head

The biaxial tensile stress σ_H, on a small circular element of the vessel head (radius δr) is given by:

$$P\pi\delta r^2 = 2\pi\delta r t_H \sigma_H \delta r / R_H \tag{C.1}$$

where P is the internal vessel overpressure, t_H is the average vessel head thickness (=15.9 mm), and R_H is the local vessel head radius of curvature (≈2 m)

$$P = 2t_H \sigma_H / R_H \tag{C.2}$$

For rupture, σ_H must be greater than the ultimate tensile strength σ_U, of the vessel material. σ_U is a function of the material composition, its history (such as any heat treatment) and temperature at rupture. A value of 30 tons/in.^{2} (465 MPa) is typical for weldable structural steels (e.g. EN2) up to 300°C. Hence:

$$P_{\text{HEAD RUPTURE}} \geq 2t_H \sigma_U / R_H \tag{C.3}$$

$$P_{\text{HEAD RUPTURE}} \geq 7.4 \text{ MPa } (\approx 74 \text{ bar})$$

C1.2 Rupture of vessel wall

By contrast, for rupture of the vessel wall, it is the hoop stress in the reaction vessel wall σ_W, that must exceed σ_U:

$$P2R_W\delta h = 2t_W \delta h \sigma_W \tag{C.4}$$

where t_W is the average vessel wall thickness (13.8 mm), R_W is the vessel wall radius of curvature (1.25 m) and δh is an axial (ring-shaped) element of the vessel wall.

$$P = t_W \sigma_W / R_W \tag{C.5}$$

$$P_{\text{WALL RUPTURE}} \geq t_W \sigma_U / R_W \tag{C.6}$$

$$P_{\text{WALL RUPTURE}} \geq 5.1 \text{ MPa } (\approx 51 \text{ bar})$$

Thus the actual rupture of the vessel would be expected to be in the wall, at an internal pressure not less than 51 bar.

C2 Propagation of cracks following rupture

Following the initial rupture, cracks will propagate around the vessel provided the strain energy released by the crack front advancing a distance δa exceeds the surface energy required to produce the additional crack surfaces. This section considers cracks propagating axially (down the side of the vessel) or radially (around the circumference of the vessel). Both directions of cracking occurred on the reaction vessel; the removal of the top of the vessel required largely circumferential cracking, whilst the body of the vessel was split open by axial cracking.

C2.1 Axial (longitudinal) crack

$$G t_W \delta a \leq 2\pi R_W t_W \delta a(\sigma_W^2/E) \tag{C.7}$$

where G is the surface energy per unit area of crack, E is the Young's modulus ($\approx$210 GPa for steel) and σ_W is the hoop stress in the vessel wall.

$$G = K_{IC}^2/E \tag{C.8}$$

where K_{IC} is the critical stress intensity factor for the material. Like σ_U, K_{IC} depends on the material composition, history and temperature, larger values of K_{IC} indicating more ductile materials. For the weldable structural steel considered above (EN2), $K_{IC} \approx 100$ MNm$^{-3/2}$ at 300°C. Equations (C.5), (C.7) and (C.8) yield:

$$P_{\text{AXIAL PROPAGATION}} \geq (t_W K_{IC})/(\sqrt{\pi} R_W{}^{3/2}) \tag{C.9}$$

$$P_{\text{AXIAL PROPAGATION}} \geq 0.56 \text{ MPa } (\approx 5.6 \text{ bar})$$

C2.2 Radial (circumferential) crack

Considering a circumferential crack propagation around the vessel wall:

$$G t_W \delta a \leq h t_W \delta a/(\sigma_A^2/E) \tag{C.10}$$

where σ_A is the axial tensile stress in the vessel wall, and h is the length of vessel wall relieved by the crack opening (taken to be the distance from the head weld to the top of the cooling water coil $\approx$400 mm).

The axial stress in the vessel wall is given by:

$$P\pi R_W^2 = 2\pi R_W t_W \sigma_A \tag{C.11}$$

Combining eqs. (C.8), (C.10) and (C.11) gives:

$$P_{\text{RADIAL PROPAGATION}} \geq (2\sqrt{2} t_W K_{IC})/(R_W \sqrt{h}) \tag{C.12}$$

$$P_{\text{RADIAL PROPAGATION}} \geq 4.9 \text{ MPa } (\approx 49 \text{ bar})$$

The estimated rupture pressure is therefore sufficient to account for both observed directions of crack propagation. It should be noted, however, that the internal pressure in a vessel will reduce very rapidly following the initial rupture. The internal pressure (and associated strain in the vessel wall) required for crack propagation must be maintained throughout the progress of the crack. Thus, for the almost complete removal of the vessel head, crack propagation must have been rapid and the internal pressure at rupture must have been somewhat higher than the 49 bar estimated above.

C3 Energy dissipated in crack formation

The total energy dissipated in crack formation, E_C, is given by:

$$E_C = L_C t_W G = L_C t_W K_{IC}^2 / E \qquad \text{(C.13)}$$

where L_C is the total length of crack, approximately 8 m for a complete circumferential crack and 3 m for a full length axial crack.

$$E_C \approx 7.2 \text{ kJ}$$

C4 Bending of steel beam

This section concerns the bending of a beam beyond the elastic limit. The beam in question supported corrugated sheeting. The radius of curvature R_C of a beam (at the neutral axis) is given by:

$$R_C = EI/M \qquad \text{(C.14)}$$

where E is the Young's modulus (≈ 210 GPa), M is the external bending moment, given by:

$$M = 0.25FL \qquad \text{(C.15)}$$

F is a concentrated load at the centre of the beam span, L is the span length ($=4.75$ m), I is the second moment of inertia about the neutral axis:

$$I = \int w(r) r^2 \mathrm{d}r \qquad \text{(C.16)}$$

$w(r)$ is the profile of the beam perpendicular to the plane of bending. For the L-shaped beam:

$$w(r) = 0.06 \text{ m} \quad \text{for} \quad 0.12 \text{ m} < (n+r) < 0.13 \text{ m}$$

$$= 0.01 \text{ m} \quad \text{for} \quad 0 < (n+r) < 0.12 \text{ m}$$

$$= 0 \quad \text{for} \quad (n+r) < 0 \quad \text{or} \quad 0.13 \text{ m} < (n+r)$$

n is the distance of the neutral axis from the inner edge, and r is measured outwards from the neutral axis.

Minimising I (to determine the position of the neutral axis) leads to:

$n = 0.0817$ m (i.e. 8.17 cm from inner edge)

$I = 3.135\ 10^{-6}\ \mathrm{m}^4$

The maximum stress in the beam is a compressive stress at the inner edge, given by:

$$\sigma_{max} = En/R_C \qquad (C.17)$$

For plastic yielding, σ_{max} must exceed the yield stress σ_Y. For a typical hardened steel ($Hv \approx 500\ \mathrm{kg/mm^2}$), $\sigma_Y \approx 1.6 \times 10^9\ \mathrm{Nm^{-2}}$. However, this neglects the probability that the inner edge of the beam will relieve the local stress by buckling. Thus a more realistic criterion for the onset of plastic bending is when the tensile stress at the outer edge of the beam, σ_T, exceeds the yield stress. That is:

$$\sigma_T = E(0.13 - n)/R_C \geq \sigma_Y \qquad (C.18)$$

$R_C \leq 6.34$ m

The corresponding deflection of the beam δ, is given by:

$$(2R_C - \delta)\delta = (L/2)^2 \qquad (C.19)$$

$\delta \approx L^2/8R_C = 0.44$ m

On substituting eqs. (C.14)–(C.16) into eqn (C.18), the concentrated force required for tensile yielding of the outer edge of the beam F_Y is:

$$F_Y \geq 4I\sigma_Y/(0.13 - n)L \qquad (C.20)$$

$F_Y \geq 87$ kN (≈ 8.7 tonnes)

If the force were evenly distributed, the total force for yielding would be doubled to 175 kN (≈ 17.5 tonnes). In order to obtain an estimate of the overpressure δP_C at this point, the force must be divided by the area of corrugated sheeting supported by the beam (2 m high along all of length L):

$\delta P_C = 18$ kPa (≈ 180 mbar)

It should be noted that this calculation does not allow for any bending strength on the part of the corrugated sheeting bolted to the beam.

C5 Broken door bolt

C5.1 Visual description

This section concerns a door at the rear of Building 70b at Thornton Research Centre. The one and a half standard width door was pulled outwards by the pressure wave from the explosion, breaking a bolt of circular section with 1/2″ (12.7 mm) diameter. From a visual examination only, it appeared to have suffered some plastic deformation on one side from impact with the door frame, followed by brittle fracture. The grey and multi-faceted appearance of the fracture surface indicates that the material is a malleable or ductile cast iron.

C5.2 Impact energy

The fracture of the door bolt may be considered with reference to the "Charpy V-Notch Test". In this a 10 mm square section notched bar is supported between two supports 40 mm apart. The centre of the bar is struck by a pendulum to produce fracture. The energy lost by the pendulum is equivalent to the fracture energy of the specimen.

The same test can be carried out using unnotched specimens. In the case of a ferritic ductile cast iron at ambient temperature, this yields fracture energies of 150 ± 20 J, over a wide range of material composition.

To estimate the fracture energy of the door bolt, it is necessary to scale the Charpy value by the area of the bolt:

$$E_B = (\pi/4)(d/0.01)^2 E_C \tag{C.21}$$

where E_B is the fracture energy of the bolt, E_C is the Charpy fracture energy (≈ 150 J), and d is the diameter of the bolt (0.0127 m).
This energy is provided by the overpressure δP_B acting on the door:

$$E_B = \delta P_B (A/2) s \tag{C.22}$$

where A is the area of the door (≈ 2.4 m^2) (the factor of two is to allow for the door being supported at one side by hinges), and s is the distance of action of the pressure, comprising the thickness of the bolt and the maximum free movement of the door when bolted ($\approx 2d$)

$$\delta P_B = E_C (\pi/4)(d/0.01)^2 / Ad \tag{C.23}$$

$$\delta P_B \approx 6.3\ 10^3 \text{ Pa } (\approx 63 \text{ mbar})$$

Appendix D

Thornton Research Centre Damage from fluoroaromatics plant explosion

This is a revised list of the damage. It gives a reasonable impression of the level and types of damage. In all, some 119 panes of glass were broken, and not all of these are recorded below. The damage location is marked on Fig. 4:

(1) Substantial pieces of pipe lagging.

(2) Four inset metal doors in "roller" doors pushed inwards. The frames of all four doors were bent. The doors were parallel to the fence. The nature of the plastic deformation and tear suggested a long pressure pulse. The duration must also have been at least 30 ms to have time to move the doors on their free swing far enough to start damaging them. There was no sign that the doors had been pulled outwards afterwards, but it would have been harder to pull out than push in.

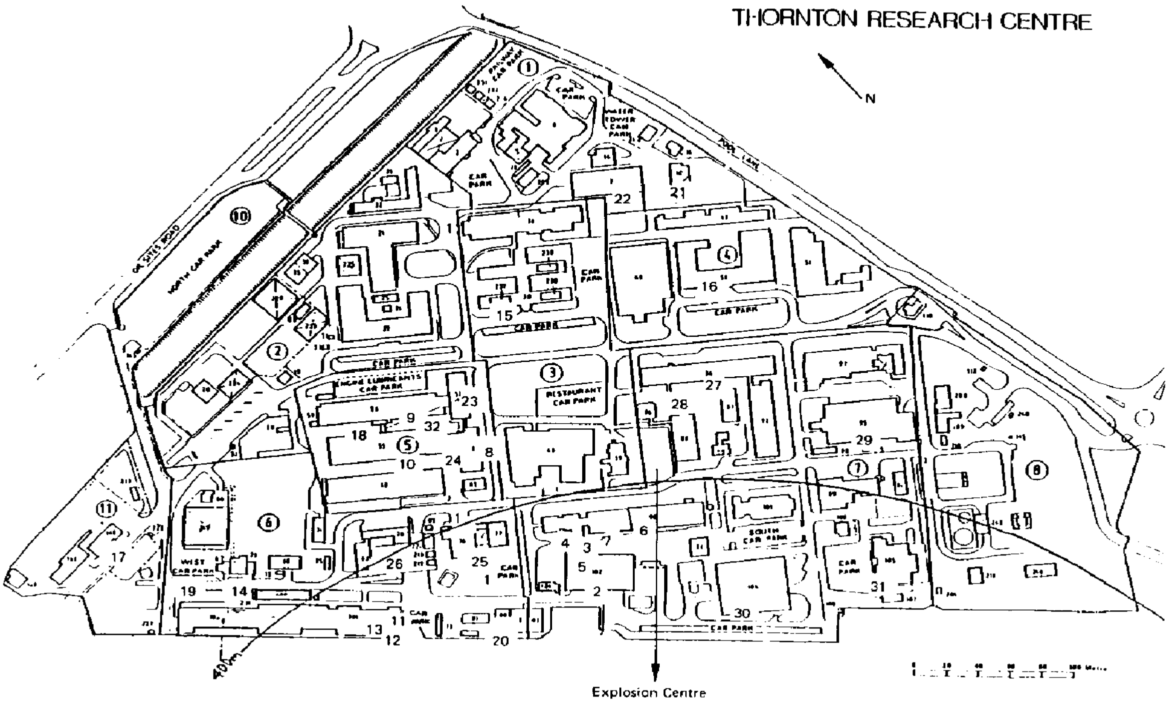

Fig. 4. Map of damage to Thornton Research Centre.

A nearby door of similar construction, perpendicular to the fence, was undamaged (although very slightly more sheltered), which suggests some directional blast.

This kind of damage to these inset "roller" doors occurred elsewhere on site (see below) and was probably caused by a force of about 5 kN, which corresponds to an overpressure of about 50 mbar. The design of these doors makes them particularly susceptible to overpressure damage.

(3) A set of fire doors had been forced open outwards. Not much force would be required to do this, but it is evidence of rarefaction.

(4) Two light covers inside the building had come off (very close to fire doors in (3)). Although the light covers were very light, and could have been lifted easily, trying to knock them back out of their fittings showed that this was not likely. Being sucked out (and flexing) due to rarefaction is more likely, and also would not have required much force.

(5) A strip light fitting had fallen down. It is impossible to work out the reason with certainty, but it was probably building shake.

(6) The detonation room is constructed with "blow-out" panels, which should vent any internal explosion. Two of these panels had partly blown out (i.e., sucked from outside). We have tested these panels and found that the movement corresponded to a force of 1 kN on small panels, which corresponds to an underpressure of 60 mbar.

(7) Two filmed windows cracked. Erratic damage is hard to quantify. Impossible to say whether it was rarefaction or compression. The windows faced in the direction of the fence.

(8) Two large wire-reinforced windows torn out of their frames outwards. The windows were door-sized. The frames had deformed by about a foot. All the nearby windows of a similar type (31 of such) were bent outwards slightly, and rendered unsafe. Eight of the 32 panes of wired glass were broken. Damage was by rarefaction, but construction meant that they would be much more sensitive to rarefaction than compression. The windows were perpendicular to the fence.

(9) Fourteen window panes just below roof level cracked. Cracking was associated with frames bending outwards. The forces required to do this were not large. The windows were parallel to the fence.

(10) Three steel doors pushed inwards, deformed by about 9 inches. Similar force required to those in (2), but doors were further from fence and sheltered from direct blast. One pair of timber doors were pulled out, damaging slip bolts.

(11) Three out of four 1 m×1 m windows broken. All small windows intact. Should be able to calculate angle to blast. No glass left the windows, and it is impossible to assess if damage was inwards or outwards.

(12) Four out of 12 small windows broken, glass outwards. It is impossible to tell if this damage was present before the explosion.

(13) A door was ripped outwards. The damage of the door locks was considerable. The top bolt was bent and then snapped. The bottom bolt was bent and ripped the corner of the door off. The top bolt has been analysed (Appendix C) and had a yield energy of 150 J. Allowing for the lower bolt damage, this gives an energy density of at least 100 Jm^{-2} for the rarefaction phase of the blast (which is considerable at the distance). An underpressure of around 65 mbar is indicated. A total energy of at least 500 MJ is implied. (150 J of rarefaction energy on one of two door bolts 375 m away implies a rarefaction energy density of 250 $\mathrm{J/m^2}$ over a 375 m radius hemisphere, which gives an energy yield of 220 MJ just in rarefaction, implying at least 500 MJ total: although this figure is calculated from a single door bolt, it is consistent with the level of rarefaction underpressure estimated from elsewhere at Thornton.)

(14) A heavy 3 m door ripped four screws and two nails from its bolt outwards. Although the force required to do this was reasonable, the door area was large, and the required overpressure was small.

(15) One glass panel broken. One first floor window frame bent inwards, one second floor window frame bent outwards.

(16) Four glass panels cracked (rooms 6, 7, 28 and 29).

(17) One window cracked.

(18) Draught-proofing on door moved outwards.

(19) Draught-proofing on garage door moved outwards.
(20) Fire door opened outwards.
(21) Two glass panels cracked
(22) Six window panes cracked.
(23) Glass-fronted door cracked.
(24) West-facing roller door pushed inwards. Similar to damage in (2) and (10).
(25) Three glass panels broken.
(26) Glass door panel broken.
(27) Five glass panels broken.
(28) One window cracked.
(29) Cladding cracked and damaged. Timber doors sucked outwards. One window frame pushed in.
(30) Ceiling tiles blow out. One pair of double doors blown out, bolts damaged.
(31) External door lifted out of track.
(32) Roller shutter door damaged inwards. The other doors damaged outwards.

Appendix E

Reactor Data 20 March 90

Time	Reactor temperature (°C)	Jacket temperature (°C)	Reactor pressure (barg)
2:50	149.8	160	0.218
2:51	150.4	160	0.225
2:52	151.0	160	0.234
2:53	151.5	160	0.246
2:54	152.0	160	0.261
2:55	152.7	160	0.280
2:56	153.2	160	0.299
2:57	153.8	160	0.323
2:58	154.4	160	0.349
2:59	154.9	160	0.376
3:00	155.5	160	0.404
3:01	156.2	160	0.438
3:02	156.9	160	0.479
3:03	157.5	160	0.524
3:04	158.2	160	0.574
3:05	159.0	160	0.626
3:06	159.9	160	0.686
3:07	160.8	160	0.755
3:08	161.8	160	0.831
3:09	163.0	160	0.929

Appendix E (continued)

Time	Reactor temperature (°C)	Jacket temperature (°C)	Reactor pressure (barg)
3:10	164.4	160	1.031
3:11	165.7	160	1.146
3:12	167.6	160	1.203
3:13	169.4	159	1.435
3:14	171.6	156	1.614
3:15	174.2	150	1.844
3:16	177.2	144	2.113
3:17	180.6	139	2.473
3:18	185.0	132	2.976
3:19	190.3	130	3.675
3:20		Data lost	

Appendix F: Jet fire tests on light fittings

An element of the investigation concerns Missile 47, a 4′ twin-tube light fitting that is believed to have been ejected from the plant. It is not clear whether this was an active or redundant unit.

This appendix describes an investigation of the damage and associated experimental work that was carried out in a number of stages.

F1 Examination

The following observations are from examination of Missile 47. For convenience, the locations of features are referred to Fig. 5; the orientation indicated is arbitrary and is not intended to relate to its original orientation.

The unit was essentially intact; the right-hand half was fire-damaged. On

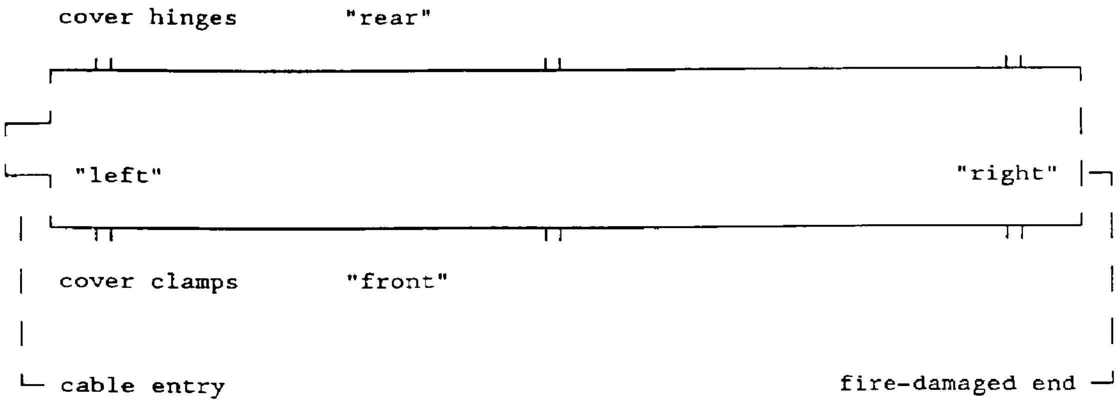

Fig. 5. Sketch plan of Missile 47.

receipt, the left-hand and central cover clamps were unfastened and the cover partly open.

The GRP casing had not suffered significant mechanical damage but a quite compact area of about 100 cm^2 at the right-hand end, extending around the sealing channel towards the right-hand cover clamp, had been burned to the extent that essentially all the resin had been lost, leaving an incoherent mass off glass fibre. This had little mechanical stiffness and was soft to touch.

The right-hand half of the cover had been burned and distorted and had partially collapsed. At the right-hand and there was an irregular hole, approximately 1 cm$\times$2 cm. This had rounded (burned) edges, i.e. it did not have sharp, clean edges that would be expected to result from an impact fracture. The interface between the burned portion of the cover and the unaffected region was very distinct with a relatively small band of sooting.

Approximately 50 cm of the thin, outer layer of the metal securing band that fits around the periphery of the cover was missing. At the right-hand end it appears that it might have been burned away; at its left-hand end (near the centre of the front edge) it had been fractured or torn.

When the remaining cover clamp was released it was apparent that the right-hand end of the cover had become fused to the internal components. In order to release the major portion, a transverse saw cut was made at approximately 24 cm from the right-hand end to initiate a fracture which separated the required section. The adhering rubber seal was also cut in three places to secure final release.

It was noted that the front tube was broken: part of it being attached to the cover. It is fairly certain that this break was not caused by removing the cover although the damage may have been made slightly more extensive in this operation. The rear tube had remained intact, surviving the blast and subsequent impact on landing.

The rubber sealing strip had been incorrectly seated in two places toward the left-hand end; one at the front flange and one at the rear. The permanent set and witness marks indicate that it had been so fitted for some time. This would likely have impaired the explosion-proof rating of the unit.

F2 Exposure to jet fire

In order to determine what form and duration of fire had caused damage to the cover, an experiment to subject lighting units to direct flame impingement and to radiation only was set up.

An attempt was made to generate comparable damage to two similar CEAG units by exposure to a 7 MW propane jet flame. One was partially engulfed by the flame with half of the cover subjected to direct impingement at about 4 m from the jet source. The heat flux within the impinging flame would be of the order of 200 kW m^{-2}, with approximately 50% radiative and 50% convective. The other unit was positioned approximately 1 m from the edge of the flame envelope, receiving radiate heat only, estimated to be at least 20 kW m^{-2}, with half of the cover shielded by a board. Both lighting units were exposed in Test 1, in which the engulfed unit became severely damaged, whereas the other was visually unaffected. The damaged unit was removed for Test 2, in which the flame was allowed to burn for a longer period.

Test 1

The fittings were exposed to the jet fire for 25 s. From end to end of the impinged cover there was a complete range of effects from total destruction to unaffected. In the region where the edge of the flame envelope had impinged on the cover, there was a transition zone of about 150 mm containing whitened and charred material. It is estimated from the video recording that a degree of damage comparable to that on Missile 47 was achieved in 12–17 s.

Test 2

The appearance of the irradiated cover after 3 min exposure to thermal radiation was totally different to that in the impingement experiment. There was no swelling or charring of the surface. It had softened and collapsed, leaving a glossy surface with some small blisters. In further contrast to CEAG unit 1, the interface with the unaffected region that had been shielded by the board was sharp (about 15 mm wide).

The interface between damaged and undamaged portions of Missile 47 had some quite sharp delineations suggesting that the unaffected half was shielded to a certain extent. The soot pattern tended to support this. The affected surface, however, had an appearance more akin to that seen during flame engulfment of CEAG unit 1. At this stage, it was concluded that Missile 47 had been exposed to short-duration partial direct impingement of a flame rather than longer exposure to radiation from a nearby flame.

F3 Analyses

Samples of the cover material of Missile 47 were subjected to infrared and Raman spectroscopy, and both techniques give spectra that were consistent with those of polymethyl methacrylate polymer, PMMA (e.g. “Perspex”). We had some difficulty in obtaining additional examples of units with this cover, since the use of PMMA was discontinued 7–8 years ago. Eventually, two similar units were located and analyses of the covers confirmed PMMA. One of these units was used in Test 3, and a second in a blast-loading test.

The casing of each unit was analysed using pyrolysis techniques. It was presumed that all the casings were constructed from the same type of polyester composite; the results supported this.

F4 Exposure to small flame

Evidence from the casing of Missile 47 suggested that impingement of a smaller, highly directional flame, aligned essentially along the major axis of the unit, was a credible source. An acetylene torch was used to produce a luminous, sooty diffusive flame of about 0.7 m in length. The radiant component of heat flux from this flame was about 150 kW m^{-2}; the total flux could not be determined because of excessive soot deposition on the monitoring instrument.

Test 3

The lighting unit was supported horizontally with the transparent cover uppermost. Although this almost certainly bore no relationship to the orientation of the original unit, if offered the best view of the critical parts in this test.

The torch was hand-held and directed onto the corner of the casing in line with the sealing channel and at a small angle to the main axis of the unit, aiming towards its centre. This caused the flame to engulf most of the end of the unit and to wash over the cover.

The dense nature of the flame prevented much observation of the behaviour of the target, either directly or from the video recording, and it was not possible to determine when the various components ignited. A soot layer was established on the cover at between 5–10 s. After 25 s, there was definite evidence that both casing and cover were alight and at that point the torch was removed. Residual flames were extinguished with a dry powder extinguisher.

The cover had partially collapsed in a similar manner to that of Missile 47. A small hole of about 2×3 cm had formed at the end of the cover. The resin of the GRP casing had burned to an extent that the reinforcing fibres could be readily separated. At the edge of the sealing channel it had burned through, as on Missile 47.

No thermal radiation experiments were conducted on units with a PMMA cover. In light of the previous work, it is inconceivable that the associated intensive damage to the casing could be achieved in a reasonable time frame without flame impingement.

F5 Conclusion

Fire damage comparable to that observed on Missile 47 has been created on a similar lighting unit by impingement of a highly directional, energetic flame of modest proportions for 25 s. Damage to the casing and the cover, which are made of different materials, is a close match to that observed on the original.

Appendix G

Potential energy yield from DFA reactor

The aim here is to calculate the heats of decomposition of the materials present in the CFA reactor at the time of the explosion. The calculation is necessarily crude, at insufficient data on the products of decomposition have been found.

G1 Dichloronitrobenzene

The problem here is that both the heat of formation of 2,4-dichloronitrobenzene and its decomposition products are unknown. The heat of formation of the material in its standard state (i.e. solid) was estimated by inference from the known heat of formation, see Ref. [G1], of 1,4-difluoro-2-nitrobenzene of −79.4 kcal/mol. The difference between the two molecules is in the position of the halogen groups and in the substitution of two chlorine for two fluorine molecules. Taking the second problem first, the differences between the heat of formation of several fluoro-substituted compounds and their corresponding chloro-analogues, expressed per Ar–X bond, are given in Table G1.

The last figure in the list comes from Benson's Ref. [G2] tabulation of group additivity functions. Note that the values are all quite close to each other, even when other functional groups are present, except for the case of *o*-fluorotoluene, presumably due to a longer range interaction between $-CH_3$ and –F and/or –Cl. Taking the value of 37.5 kcal/mol as realistic, leads to a heat of formation of 1,4-dichloro-2-nitrobenzene of −4.4 kcal/mol. Furthermore, the differences between the heats of formation of 1,2-difluorobenzene, 1,3-difluorobenzene and 1,4-difluorobenzene are fairly small, around 5%, so we will assume that the arrangement of molecules around the ring is a second-order effect. Hence, the standard heat of formation of solid 2,4-dichloronitrobenzene is assumed to be −4.4 kcal/mol.

The prediction of the products of the decomposition is much more difficult. Taking as example, the decomposition of TNT, the actual value is not calculable by simple chemistry, because as many as 23 different products can be

TABLE G1.

Heats of formation of fluorocarbons per Ar–X bond

Fluorinated compound	(Ar–Cl)-(Ar–F) (kcal/mol)
Hexafluorobenzene (g)	36.7
m-Difluorobenzene (l)	38.6
Fluorobenzene (l)	38.7
m-Fluorobenzoic acid (s)	37.7
o-Fluorotoluene (l)	30.6
p-Fluorotoluene (l)	39.9
$(C_B-Cl)-(C_B-F)$	39.0
Average	37.5

found [G3]. The approach used here is to write down plausible overall reactions and examine their energy yield to determine a realistic value, e.g.

$$C_6H_3Cl_2NO_2 \rightarrow 2HCl(g) + 1.5CO(g) + 0.5H_2O(g) + 0.5N_2(g) + 4.5C(s)$$

$$\Delta H = -108 \text{ kcal/mol}$$

$$\rightarrow 2HCl(g) + 0.75CO_2(g) + 0.5H_2O(g) + 0.5N_2(g) + 5.25C(s)$$

$$\Delta H = -139 \text{ kcal/mol}$$

Clearly, the molecule is deficient in oxygen and so much of the potential energy is not released. None the less, formation of two HCl molecules releases a considerable amount of energy. Other reactions can be written to form alternative small hydrocarbons, e.g. formaldehyde, and the net energy release would then be lower. Taking a value of say 100 kcal/mol, gives a potential energy release for anaerobic decomposition of 2.17 MJ/kg. A more reliable estimate could be obtained by performing an equilibrium calculation considering more of the candidate products, but with much more effort.

G2 4-Fluoro-2-chloronitrobenzene

This is a product of the Halex reaction and so would be expected to be present. Taking an analogous approach to that above, the heat of decomposition for the two corresponding reactions is −112 and −143 kcal/mol, respectively. Thus, the dichloro and the fluorochloro can be treated as essentially the same in terms of their heats of decomposition.

G3 Dimethylacetamide

The heat of formation of dimethylacetamide (g) was calculated, using Benson's group additivity tables, to be −57 kcal/mol. Thus, the heat of decomposition of this molecule will be negligible, and probably endothermic. Furthermore, the heat of hydrolysis to acetic acid and dimethylamine will be essentially zero.

G4 Heat of combustion of 2,4-dichloronitrobenzene

As a rough estimate (to within about 10%), the heat of combustion of 2,4-dichloronitrobenzene can be calculated assuming the combustion products are CO_2, N_2, Cl_2 and H_2O. This gives a figure of around 2.8 MJ/mol, or 14.5 MJ/kg.

G5 References

G1. D.R. Stull, E.F. Westrum and G.C. Sinke, The Chemical Thermodynamics of Organic Compounds, Kreiger, Malabar, FL, 1989.
G2. S.W. Benson, Thermochemical Kinetics, J. Wiley, New York, NY, 1968.
G3. Kirk-Othmer Encyclopaedia of Chemical Technology, Wiley–Interscience, New York, NY, Vol. 3rd edn., 1986.